Journal of *Marine Science and Engineering*

MDPI

Article

An Intelligent Monitoring System for the Force Characteristics of Floating Bollards in a Ship Lock

Linjian Wu [1], Jia Yang [1,*], Zhouyu Xiang [1,*], Mingwei Liu [1], Minglong Li [2], Yutao Di [1], Han Jiang [1], Chuan Dai [1] and Xudong Ji [1]

[1] National Engineering Research Center for Inland Waterway Regulation, School of River and Ocean Engineering, Chongqing Jiaotong University, 66 Xuefu Road, Nan'an District, Chongqing 400074, China; linjian_wu@cqjtu.edu.cn (L.W.); mingwei_liu@cqjtu.edu.cn (M.L.); diyutao@mails.cqjtu.edu.cn (Y.D.); jianghan@mails.cqjtu.edu.cn (H.J.); daichuan@mails.cqjtu.edu.cn (C.D.); jixudong@mails.cqjtu.edu.cn (X.J.)

[2] Sichuan Communication Surveying and Design Institute Co., Ltd., Chengdu 610017, China; minlonli@126.com

* Correspondence: jia_yang@mails.cqjtu.edu.cn (J.Y.); xzy@mails.cqjtu.edu.cn (Z.X.)

Abstract: Due to the large scale of navigation ships, the fast speed of entering the lock, and the irregular mooring and the complicated flow conditions in the lock chamber, it is common for the floating bollards of the lock to suffer structural damage or even failure due to the overloaded mooring force. However, the traditional cable load measurement method cannot offer real-time feedback on force characteristics of floating bollards, making it difficult to accurately judge its service status. To this end, according to the floating bollard structure type and load condition of a representative ship lock project in China, this paper determines the theoretical model parameters of a floating bollard load response based on three-dimensional finite element numerical simulation test data and constructs a modified load response model of floating bollards. On this basis, an intelligent floating bollard monitoring system based on big data, internet, and cloud services is developed to intelligently perceive real-time floating bollard force characteristics and monitor the long-term service status. Relying on a representative ship lock in China, a field test of the floating bollard intelligent monitoring system is carried out. The relative error between the calculated values via the model (i.e., system exhibition results) based on the numerical results and the field-measured values is within 15%. This result verified the accuracy and effect of the monitoring system. This research supports the establishment of the digital perception monitoring platform for ship lock facilities and improves the automation level of ship lock operation and management as well as overall risk prevention and control capabilities.

Keywords: ship lock; floating bollard; force characteristics; intelligent monitoring; system development

Citation: Wu, L.; Yang, J.; Xiang, Z.; Liu, M.; Li, M.; Di, Y.; Jiang, H.; Dai, C.; Ji, X. An Intelligent Monitoring System for the Force Characteristics of Floating Bollards in a Ship Lock. *J. Mar. Sci. Eng.* **2023**, *11*, 1948. https://doi.org/10.3390/jmse11101948

Academic Editor: Erkan Oterkus

Received: 1 September 2023
Revised: 28 September 2023
Accepted: 3 October 2023
Published: 9 October 2023

1. Introduction

With continuous improvements in navigation conditions on global waterways, the total freight volume on ships is increasing, and waterway transportation is gradually promoting the rapid integration and development of global and regional economic activity [1–3]. As key components of waterway transportation, safe and efficiently operated ship locks are important prerequisites for ensuring unimpeded waterways. According to statistics, there are a total of 1041 ship locks under construction or completed in China [4], which are generally running stably. However, there are a series of problems related to the operation and maintenance of ship locks such as risk management, the investigation, monitoring, and early warning of dangers, and emergency disposal [5]. Floating bollards are important tools used to ensure the safe mooring of ships during the rising and falling water process in a lock chamber, and their safety is an important factor when ensuring efficient lock operation [6,7]. However, due to the significant trends of large-scale ships in recent years, the excessive speed of ships entering the lock, the irregular moorings, the complex flow conditions in the lock chambers, and the blockage of the chute by floating

foreign matter, etc., a series of damages and even damage phenomena such as column breakage, guide channel deformation, and pulley blockage occur under the overloaded mooring force, resulting in the pulling/slinging of the ship into the water and causing major safety accidents such as hull damage and casualties [8–10]. Therefore, the intelligent monitoring of floating bollards in complex environments has become a major technical issue that urgently needs to be studied and addressed in the modern-day operation and maintenance management of ship locks.

At present, the traditional force measurement method of monitoring mooring line tension through the use of a force sensor installed on ship mooring lines is ineffective in obtaining the force characteristics of floating bollard structures, and it is impossible to consider the damage threshold of a floating bollard under different service conditions [11–14]. This has no supervisory initiative for the lock operation management unit. It is difficult to monitor the real-time mooring status of all ships passing through the lock and it is unattainable to achieve early warning or subsequent accountability for navigation lock safety accidents. To address this problem, a small number of domestic and overseas scholars have carried out relevant research on the force characteristics of floating bollard structures (including fixed mooring bollards on a wharf and floating mooring bollards in a ship lock). Numerical simulation was used to determine the optimal layout position of the strain monitoring point in a floating bollard structure. Wang et al. [15] established a theoretical model between a floating bollard and the mooring force of a ship. A standard mooring force inversion model for floating bollards based on the standard mooring force was established by Wu et al. [16], and a stress safety monitoring method for the floating bollard structure based on multipoint strain fusion was proposed. The feasibility and accuracy of the method were verified by analyzing the measured ship mooring force in the field test and the inverted mooring force under standard conditions. By studying the problems related to ship mooring force in the filling and emptying process of a lock chamber, a method was proposed by Mulder et al. [17] to evaluate ship mooring safety based on the permissible value for the mooring force of floating bollards. According to the mechanical characteristics of a floating bollard structure in the No. 1 ship lock of Gezhouba, the sensitive areas of the floating bollard load response were determined by Liu et al. [18–20] using the method of numerical simulations. On this basis, a mechanical model of floating bollard load response was educed if the vertical mooring angle β was considered as a positive value, and the precision of the model was proved based on the in situ experimental data in a certain ship lock in China. Wu et al. [21] proposed a dynamic inversion model for the mooring force of floating bollards based on the mathematical and mechanical basic theories. This model can convert the strain signal into mooring force information in real-time, and the precision of the model was proved through physical model tests. Furthermore, Qi et al. [22] proposed an optimal control scheme of a lock water delivery system based on the loading monitoring method of a floating bollard in a ship lock.

With the flourishing development of global computer networks and automation control technology, the automatic monitoring and early warning technology of lock navigation safety has gradually become a trending research topic [23]. Li et al. [24] proposed an online monitoring method for bollard structure force characteristics based on real-time data acquisition and transmission technology and constructed an overall framework for a bollard structure monitoring system. Li et al. [25], using the miter gate of the No. 2 lock of the Gezhouba Dam, Wuhan, China, as an example, enacted an online monitoring system to obtain the actual stress and crack signals of the gate, which was combined with an analysis of numerical simulation test data to evaluate the operational status of the actual gate. Zhang et al. [26] designed a condition monitoring system for the opposite arc valves of lock gates to monitor the operating condition of reverse arc valves. Tang et al. [27] designed a multichannel water level monitoring and SMS interaction system for lock chambers based on a high-performance W77E58 microcontroller. Misovic et al. [28] proposed a vessel detection algorithm used in an online laser monitoring system for ship locks, which significantly improved the detection accuracy of the monitoring system. Liu

et al. [29] proposed a ship navigation state and formation state perception method based on millimeter-wave radar and ship–coast interactions and established a ship cooperative formation monitoring system for ships in lock channels. The effectiveness of the system and method was verified by field tests. Hao et al. [30] designed a new type of ship bottom visual monitoring system to realize the rapid and accurate monitoring of explosives at the bottom of a ship, the damage to the bottom of the ship, and the fouling of the ship. Hu et al. [31] proposed a design scheme of an RFID-based ship management system for inland river crossing locks to realize the visualization and digital management of ships passing through locks.

In summary, the related research on the operation status testing of floating bollards in ship locks is still in the initial stage. Currently, a set of systematic, completely automated and intelligent monitoring methods and technologies has not been developed, making it difficult for management units at navigation hubs to perform the real-time and proactive supervision of ship mooring status and safety conditions of floating bollards within lock chambers. Therefore, there is an urgent need to develop an online long-term intelligent monitoring system that can reflect the force characteristics of floating bollards. To address the above problems, this paper determines the theoretical model parameters of the load response of a floating bollard by carrying out a three-dimensional finite element numerical simulation test of the main floating bollard structure to construct a modified load response floating bollard model. Following this model, an online long-term sequence active monitoring method for the service status of floating bollards in ship locks based on modernized technologies such as wireless transmission, cross-domain collaboration, and information fusion is proposed, and an intelligent monitoring system for floating bollard force characteristics in ship locks based on big data, internet, and cloud services is integrated. The testing accuracy of the monitoring system is verified through a field test at a representative ship lock in China, resulting in a comprehensive improvement in the level of intelligent operation and maintenance of critical ship lock equipment, which is of great scientific and practical value.

2. Theoretical Model of the Load Response of Floating Bollards

When a ship is moored inside a lock chamber, a horizontal angle α between the mooring line and the lock wall line and a vertical angle β between the mooring line and the horizontal plane are formed in the horizontal and vertical projection planes, respectively (see Figure 1). When the height of the ship's freeboard exceeds that of the floating bollard, it will be subjected to upward mooring force, and at this time, the vertical angle $\beta > 0$ (see Figure 1a). Conversely, the floating bollard will be subjected to downward mooring force, i.e., $\beta < 0$; see Figure 1b [21]. According to the specifications [32] and field measurements [33], β can be taken as 15° and -15° in the above two cases.

Based on the structural type and characteristics of the floating bollard, a structural system composed of a hollow cylindrical body and upper and lower stainless plates is generalized as a hyperstatic linear elastic overhanging beam model with an equal section restrained by fixed bearings. The upper and lower stainless plates are considered fixed hinge supports and fixed supports, respectively (see Figure 2) [21]. There are two test points T and K for structural strain confirmed on the surface of the hollow cylinder column for the floating bollard, as shown in Figure 1d, and the structural strains at the two points of T and K are respectively set as ε_T and ε_K. Based on previous research results from this research team [21], the fundamental theory of mathematical mechanics is used, combined with the generalized geometrical model in Figure 2b,c, the mathematical and mechanical relationships between the strain ε and the mooring force F, as well as the horizontal angle α, are quantified, and the theoretical model of floating bollard load response under the mooring force is proposed as follows:

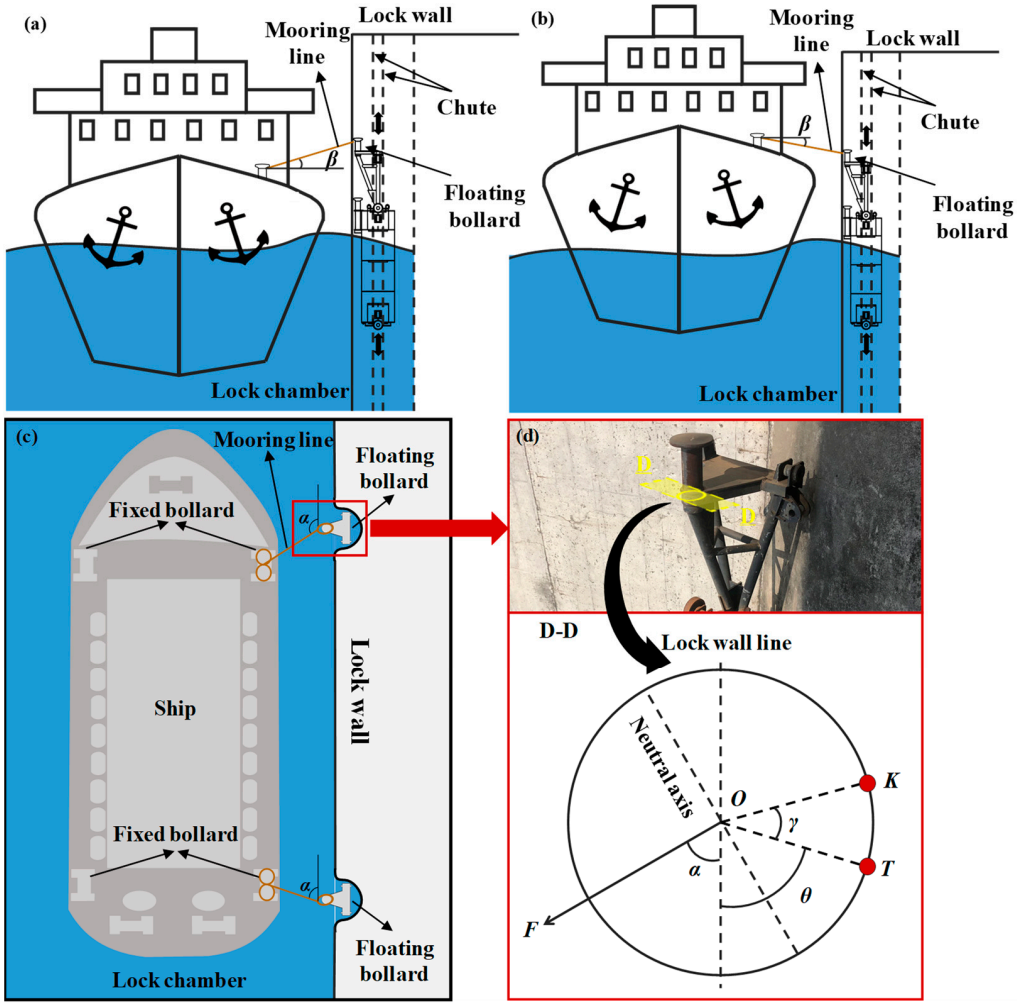

Figure 1. Mooring angle of floating bollard and location of measurement points under the ship mooring force: (**a**) $\beta > 0$ ($\beta = 15°$); (**b**) $\beta < 0$ ($\beta = -15°$); (**c**) horizontal angle α; (**d**) strain measuring point.

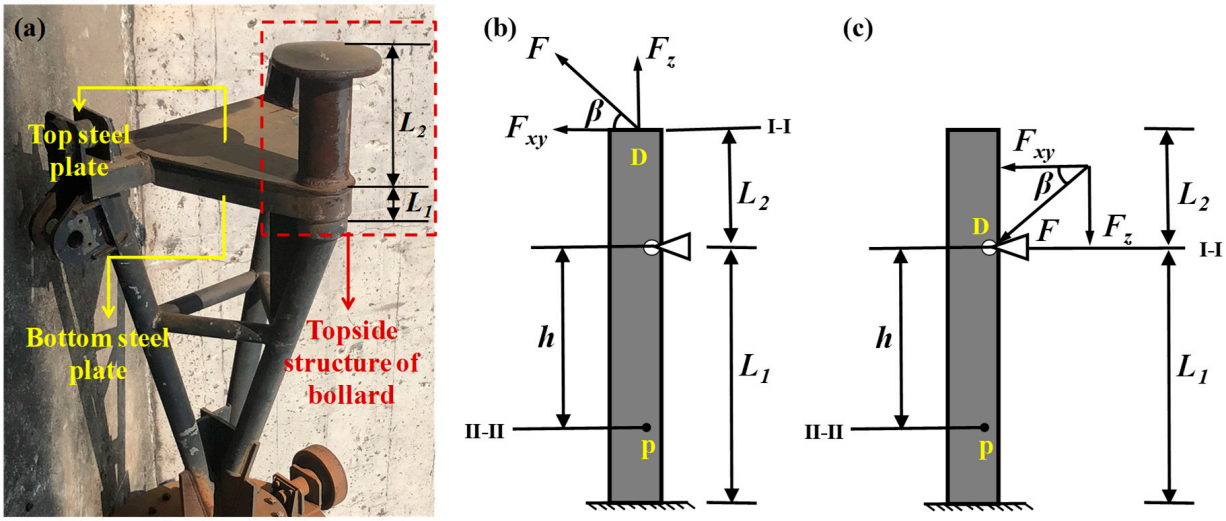

Figure 2. The floating bollard in a ship lock: (**a**) floating bollard; (**b**) generalized overhanging beam model ($\beta > 0$); (**c**) generalized overhanging beam model ($\beta < 0$) [21].

If the mooring angle $\beta > 0$, $\beta = 15^\circ$:

$$\begin{cases} \alpha(t) = \arccos\frac{0.259I_1[\varepsilon_T(t)-\varepsilon_K(t)]}{A_1R(m+n)\sqrt{x^2+y^2}} - \delta - \arctan\frac{y}{x} \\ F(t) = \frac{E_1I_1[\varepsilon_T(t)-\varepsilon_K(t)]}{R(m+n)[\cos(\alpha+\delta)-\cos(\alpha+\delta+\gamma)]} \end{cases} \quad (1)$$

where $m = 0.483(2L_1 - 3\,h)L_2/L_1$, $n = 0.518R/\pi$, $x = \varepsilon_T\,(t)\cos\gamma - \varepsilon_K\,(t)$, and $y = \varepsilon_T\,(t)\sin\gamma$; A_1 is the section area of the hollow cylinder of the floating bollard; L_1 is the length between the fixed hinge support and the fixed support of the hollow cylinder; L_2 is the length of the cantilevered section of the hollow cylinder; h is the length from the strain measurement point to the fixed hinge support; I_1 is the moment of inertia of the circle of the cross-section of the hollow cylinder; E_1 is the elastic modulus of the hollow cylinder; and R is the axial cross-section of the circle of the floating bollard radius.

If the mooring angle $\beta < 0$, $\beta = -15^\circ$:

$$\begin{cases} \alpha'(t) = \arcsin\frac{-0.259A_2L_1^3I_1[\varepsilon_T'(t)-\varepsilon_K'(t)]}{A_1R(m'-n')\sqrt{x'^2+y'^2}} - \delta - \arctan\frac{y'}{x'} \\ F'(t) = \frac{A_2L_1^3E_1I_1[\varepsilon_T'(t)-\varepsilon_K'(t)]}{R(m'-n')[\cos(\alpha+\delta)-\cos(\alpha+\delta+\gamma)]} \end{cases} \quad (2)$$

where $m' = 2.898hL_3I_1$, $n' = -0.518A_2{L_1}^3R/\pi$, $x' = \varepsilon_T'(t)\sin\gamma$, and $y' = \varepsilon_K'(t) - \varepsilon_T'(t)\cos\gamma$; L_3 is the length of the steel plate for the superstructure of the floating bollard; and A_2 denotes the section area of the steel plate for the superstructure of the floating bollard.

Based on Equations (1) and (2), the horizontal angle, i.e., α, and the mooring force, i.e., F, can be calculated according to the strain of the floating bollard. On the basis of reference [16], the generalized physical model test method for the superstructure of the floating bollard (the hollow cylinder body and the structural system composed of the upper and lower steel plates) with a model scale of 1:1 is used to verify the accuracy of the theoretical model for the floating bollard load response (Equations (1) and (2)). However, there are still some differences between the generalized physical model and actual floating bollard structure. In order to further testify the precision of the above theoretical model in a real floating bollard, in-depth related research is carried out based on the three-dimensional numerical simulation test method.

3. Model Parameter Calibration via Numerical Simulation Experiments

3.1. Three-Dimensional Finite Element Model of a Floating Bollard

According to the floating bollard of a representative ship lock in China (see Figure 3a), a three-dimensional numerical simulation model (3D NSM) of its main structure is established (see Figure 3b). The materials of each component in the model are Q235 steel, and the parameters are shown in Table 1. Considering the symmetry of the main structure of the floating bollard, the four longitudinal and transverse rollers are generalized as three-dimensional prisms, and the top cap of the floating bollard is simplified as a circular cover. The section where the strain monitoring point of the hollow cylinder body of the floating bollard is located is 170 mm above the bottom of the column body, and h = 20 mm, $\gamma = 10^\circ$, and $\delta = 80^\circ$ in Figures 1 and 2, as shown in Figure 3c.

Table 1. Material parameters of the floating bollard's topside structure.

Material	Elasticity Modulus (Pa)	Poisson's Ratio	Density (kg/m^3)	Yield Strength (Pa)	Tensile Strength (Pa)
Steel (Q235B)	2.00×10^{11}	0.30	7850	2.50×10^8	4.60×10^8

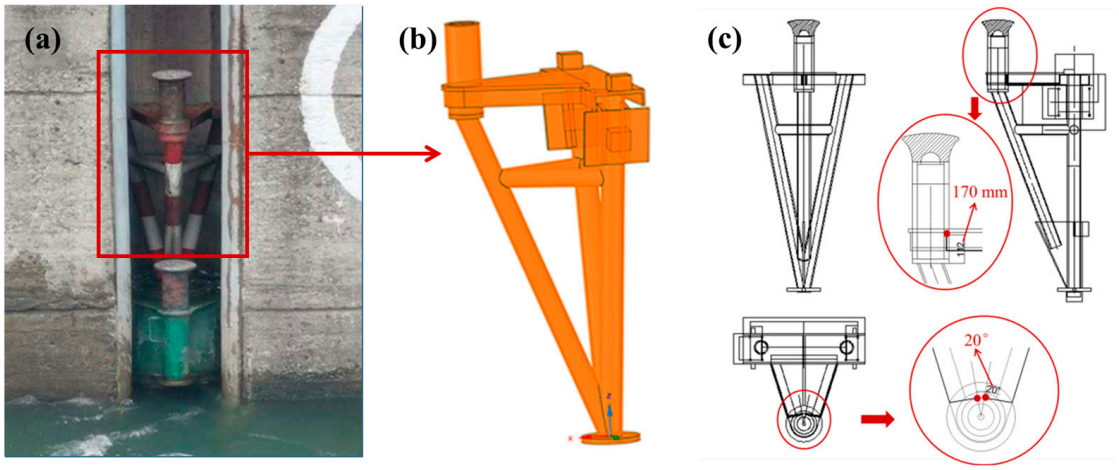

Figure 3. The floating bollard in a ship lock: (**a**) floating bollard; (**b**) 3D numerical simulation model; (**c**) locations of strain measuring points.

3.2. Numerical Simulation Test Conditions

To simulate the different mooring situations of ships passing through the lock, the loads on the main structure of the floating bollard are considered in the three-dimensional numerical simulation tests as follows:

① Structure weight, G = 3.621 kN, with the direction vertically downward.

② Water buoyancy, equal in size and opposite in direction to the structure weight.

③ Ship mooring force; there are 23 conditions: five groups of mooring force conditions (F = 5 kN, 10 kN, 30 kN, 50 kN, and 100 kN), two groups of vertical angle β conditions ($\beta = 15°$ and $-15°$), and the horizontal bollard angle α was set to start from 35° with an incremental increase of 5°, and was increased up to 145°.

The structure weight and water buoyancy are permanent loads, both of which are applied as constant loads to the 3D NSM of the main floating bollard structure. Numerical simulation calculations are carried out by combining each group of working conditions of the ship's mooring force and angle with each other, totaling 230 test conditions, as shown in Table 2.

Table 2. Numerical simulation test conditions.

α (°) / F (kN)					
β (°)	**5**	**10**	**30**	**50**	**100**
± **15**	35	35	35	35	35
± **15**	40	40	40	40	40
± **15**	45	45	45	45	45
± **15**	50	50	50	50	50
± **15**	55	55	55	55	55
.	.	.	.	.	.
.	.	.	.	.	.
.	.	.	.	.	.
± **15**	130	130	130	130	130
± **15**	135	135	135	135	135
± **15**	140	140	140	140	140
± **15**	145	145	145	145	145

3.3. Test Results and Analysis

The strain results of two monitoring points, i.e., *T* and *K*, for the floating bollard are determined on the basis of the three-dimensional numerical simulation test, as shown in Figure 4.

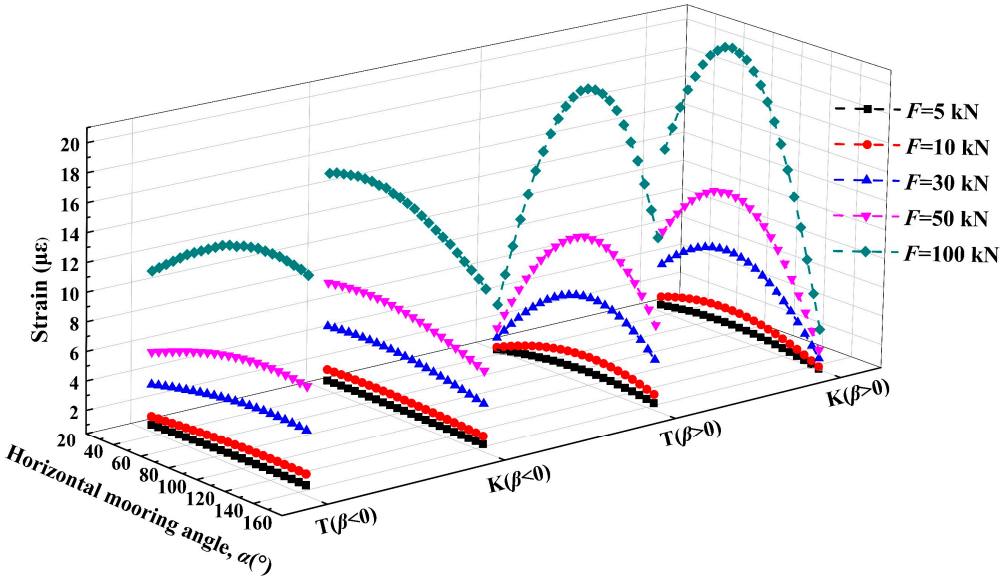

Figure 4. Test results for strain.

To verify the adaptability and accuracy of the theoretical model of the floating bollard load response in the main structure of the actual ship lock, the strain of the *T* and *K* measuring points calculated using the numerical simulation test are substituted into the theoretical model (Equations (1) and (2)). The calculated values of the theoretical model α and *F* can be calculated, which are then compared and analyzed with the preset standard values of horizontal angle α_1 and mooring force F_1 in Table 2, as shown in Figure 5. Compared with the preset standard value of the numerical simulation test, the calculated results are consistent with the trend. However, due to the difference between the hypothetical generalized overhanging beam model of the floating bollard assumed in the theoretical model and the real structure type of the floating bollard, the mooring force, i.e., *F*, and the mooring angle, i.e., α, acquired in accordance with the theoretical model have a large error compared with the true value.

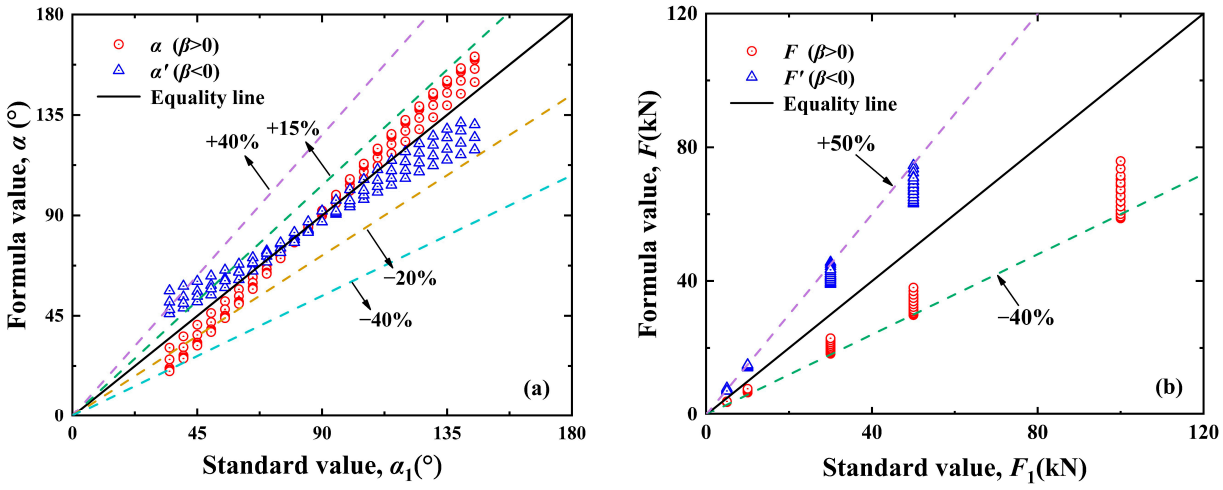

Figure 5. Calculated errors: (**a**) mooring angle α; (**b**) mooring force *F*.

To ensure the calculation accuracy of the load response model of the floating bollard, the preset standard values of α_1 and F_1 in the numerical simulation test are considered as the ordinate, the calculated values of α and F obtained via the theoretical model (Equations (1) and (2)) are considered as the abscissa, and the quantitative relationships of α~α_1 and F~F_1 are established as follows: $\alpha = \alpha(\alpha_1)$ and $F = F(F_1)$, as shown in Figure 6. The expression is as follows:

$$\beta > 0: \begin{cases} \alpha_1(t) = 0.842\alpha(t) - 8.395 \times 10^{-4}\alpha^2(t) + 3.402 \times 10^{-6}\alpha^3(t) + 17.475 \\ F_1(t) = 1.5448F(t) - 0.4877 \end{cases} \quad (3)$$

$$\beta < 0: \begin{cases} \alpha_1'(t) = 1.561\alpha'(t) - 2.65 \times 10^{-3}\alpha'(t) + 6.827 \times 10^{-6}\alpha'(t) - 30.475 \\ F_1' = 0.7669F'(t) - 1.7082 \end{cases} \quad (4)$$

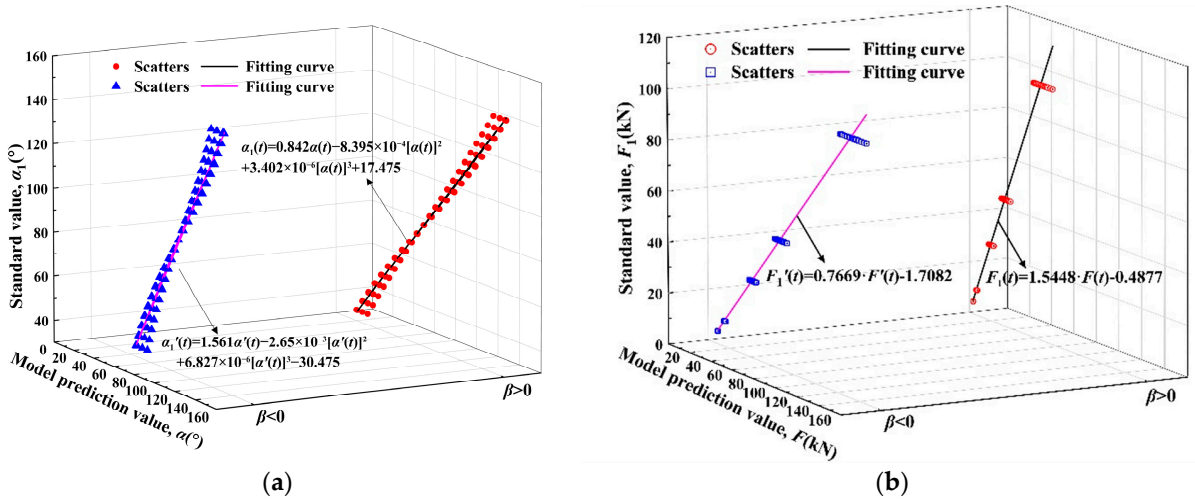

(**a**) (**b**)

Figure 6. Parameter calibration of load response model on floating bollard: (**a**) horizontal angle α; (**b**) mooring force F.

The modified floating bollard load response model can be obtained from the coupling of Equations (1)~(4), which are shown in Equations (5) and (6). Based on Equations (5) and (6), the real-time true values of the horizontal angles and mooring forces (i.e., α_1, F_1; α_1', F_1') can be obtained for the floating bollard structure under different vertical angles β. In this paper, this model (Equations (5) and (6)) is used as the core component to develop an intelligent monitoring system for the force characteristics of floating bollards in ship locks.

$$\beta > 0: \begin{cases} \alpha_1(t) = 0.842\alpha(t) - 8.395 \times 10^{-4}[\alpha(t)]^2 + 3.402 \times 10^{-6}[\alpha(t)]^3 + 17.475 \\ F_1(t) = 1.5448F(t) - 0.4877 \\ \alpha(t) = \arccos\frac{0.259I_1[\varepsilon_T(t) - \varepsilon_K(t)]}{A_1R(m+n)\sqrt{x^2+y^2}} - \delta - \arctan\frac{y}{x} \\ F(t) = \frac{E_1I_1[\varepsilon_T(t) - \varepsilon_K(t)]}{R(m+n)[\cos(\alpha+\delta) - \cos(\alpha+\delta+\gamma)]} \end{cases} \quad (5)$$

$$\beta < 0: \begin{cases} \alpha_1'(t) = 1.561\alpha'(t) - 2.65 \times 10^{-3}[\alpha'(t)]^2 + 6.827 \times 10^{-6}[\alpha'(t)]^3 - 30.475 \\ F_1'(t) = 0.7669F'(t) - 1.7082 \\ \alpha'(t) = \arcsin\frac{-0.259A_2L_1^3I_1[\varepsilon_T'(t) - \varepsilon_K'(t)]}{A_1R(m'-n')\sqrt{x'^2+y'^2}} - \delta - \arctan\frac{y'}{x'} \\ F'(t) = \frac{A_2L_1^3E_1I_1[\varepsilon_T'(t) - \varepsilon_K'(t)]}{R(m'-n')[\cos(\alpha+\delta) - \cos(\alpha+\delta+\gamma)]} \end{cases} \quad (6)$$

4. Research and Development of the System

4.1. System Overview

The intelligent monitoring system of a floating bollard in a ship lock is mainly composed of a real-time data acquisition and transmission system, a cloud computing platform, and a terminal management system, as illustrated in Figure 7. The system can perform the following three levels of functions:

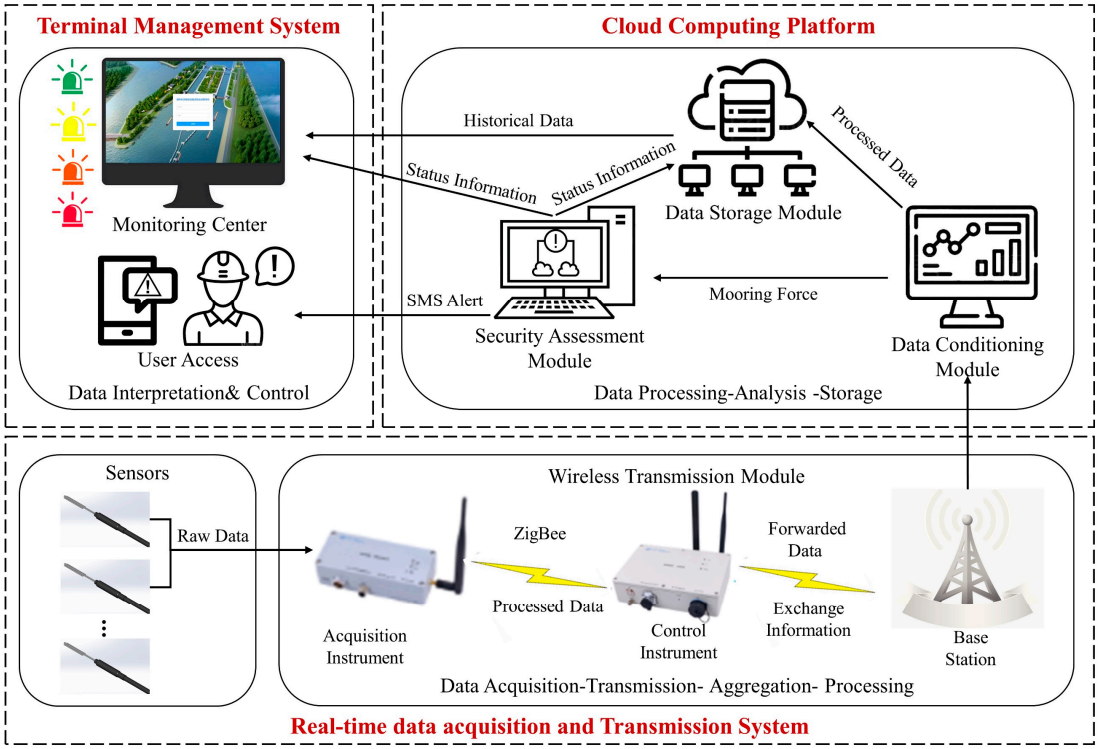

Figure 7. Topology of the system.

(1) The "perceptible" floating bollard under the normal service state, meaning that the system cloud can receive and feed important information back on the force characteristics (mooring force, angle, etc.) and operation status (whether the ship is moored, moored with several cables, etc.) of the floating bollard in real-time.

(2) The "early warning" for the floating bollard is under an extreme operating state, meaning that when the load on the floating bollard is close to a different percentage of its threshold, the system sends an early warning signal in real-time through a preset early warning mechanism to the lock management department so they can craft an emergency response.

(3) The "traceability" of the responsibility after the accident of the floating bollard is that after the safety accident on the floating bollard, the historical data stored in the cloud server of the system can be retrieved, and the accident ship can be pursued after reasonable research and judgment.

The real-time data acquisition and transmission system can collect the strain data information generated by the action of the ship's mooring force at the specified position of the hollow cylinder body of the floating bollard in real-time, and upload the collected strain data information to the cloud computing platform in real-time through the 4G network for storage and processing.

After receiving the strain data information uploaded by the real-time data acquisition and transmission system, the original strain data information is stored in the database, and then the original strain data information is extracted and substituted into the mechanical optimization model of the load response of the floating bollard. The mooring force of the hollow cylinder of the floating bollard corresponding to the strain data signal is calculated

and stored, and then the operation safety of the floating bollard is evaluated by comparing the preset threshold. Finally, the calculated ship mooring force and safety warning information are transmitted to the terminal management system for real-time display.

After receiving the ship mooring force information and the safety warning information of the operation state of the floating bollard, the terminal management system displays the load condition, operation state, and early warning information of the floating bollard in real-time through the web page, and allows users to query and download historical data.

4.2. Real-Time Data Acquisition and Transmission System

The data acquisition component includes strain sensors to measure appropriate data under varying environmental conditions, but also a wireless transmission module for the transmission of the data measured to a server in real-time. This module involves the choice, the number, and the placement of sensing modules on the structure.

4.2.1. Strain Sensor

A DH1101 welding strain gauge was selected as the monitoring sensor for the surface strain of the hollow cylinder of the floating bollard, as seen in Figure 8. The sensor has a measuring range of −3000~3000 με and an accuracy of 1 με. The sensor improves on the disadvantages of traditional pasted strain gauges, such as creep and the long curing time of strain glue. The sensitive grid was sealed in the front-end stainless steel pipe, and the stainless steel was used as the base for spot welding installation without a protective coating. The gauge can adapt to the precise long-term strain measurements of metal components in the complex environment of a lock chamber.

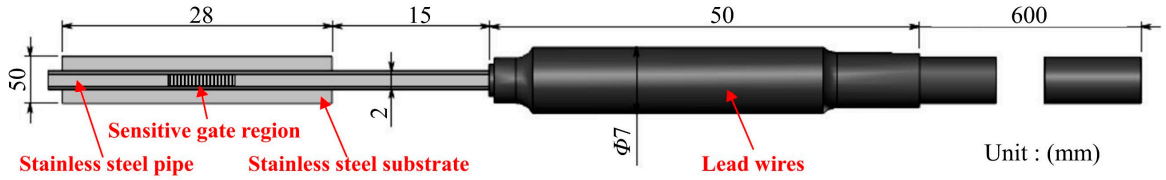

Figure 8. DH1101 welding strain gauge.

4.2.2. Wireless Transmission Module

The strain data monitoring instrument of the floating bollard was a DH2004 wireless distributed monitor, which is mainly composed of a collector, controller, and computer.

At each strain monitoring point, the collector can be distributed to collect real-time resistance signals from the strain gauge. The strain value is calculated using the sensor calibration coefficient, and the collected data signal is wirelessly transmitted to the controller through ZigBee. The controller includes a ZigBee protocol conversion module that can convert between ZigBee and 4G protocols. The controller sends data to the client through the 4G network while simultaneously amplifying, filtering, and smoothing the data signal through interpretative processing. The analog strain signal is converted into a digital strain signal, enabling the decentralized monitoring of multiple measuring points on the floating bollards within the ship lock. The system's anti-interference ability is strengthened using advanced signal isolation technology. This technology prevents weak strain signals from being disrupted by various environmental factors during long-distance transmission and prevents data information disorder or packet loss.

The strain data real-time acquisition and transmission instrument is installed on the floating bollard, which is consistently exposed to sun and rain. Environmental conditions such as wind, waves, and water flow in the lock can cause instrument failure. Therefore, the online monitoring instrument used in the strain data real-time acquisition and transmission system must have the ability to work in harsh environments for a long time and accurately upload collected strain data information to the cloud computing platform in real-time through stable wireless network data transmission technology.

4.3. Cloud Computing Platform

The cloud computing platform consists of a data conditioning module, a data storage module, and a security assessment module in order to provide an evaluation of the condition of the structure.

4.3.1. Data Conditioning Module

The data conditioning module is divided into two core processing channels:

(1) Strain-mooring force characteristic relational database: the true value of ship mooring force can be obtained quickly by matching the strain amplitude spectrum data information of the floating bollard.

(2) Based on the modified load response model of the floating bollard, the true value of the mooring force is calculated.

The specific processing process is as follows: the data conditioning module receives the digital strain signal sent by the wireless transmission module, performs spectrum analysis after conditioning and conversion, obtains the strain amplitude spectrum, matches it with the database, and if it matches, directly outputs the ship mooring force value borne by the floating bollard; if it cannot be matched, the strain data information is substituted into the modified load response model of the floating bollard to calculate the true value of the ship mooring force, as shown in Figure 9.

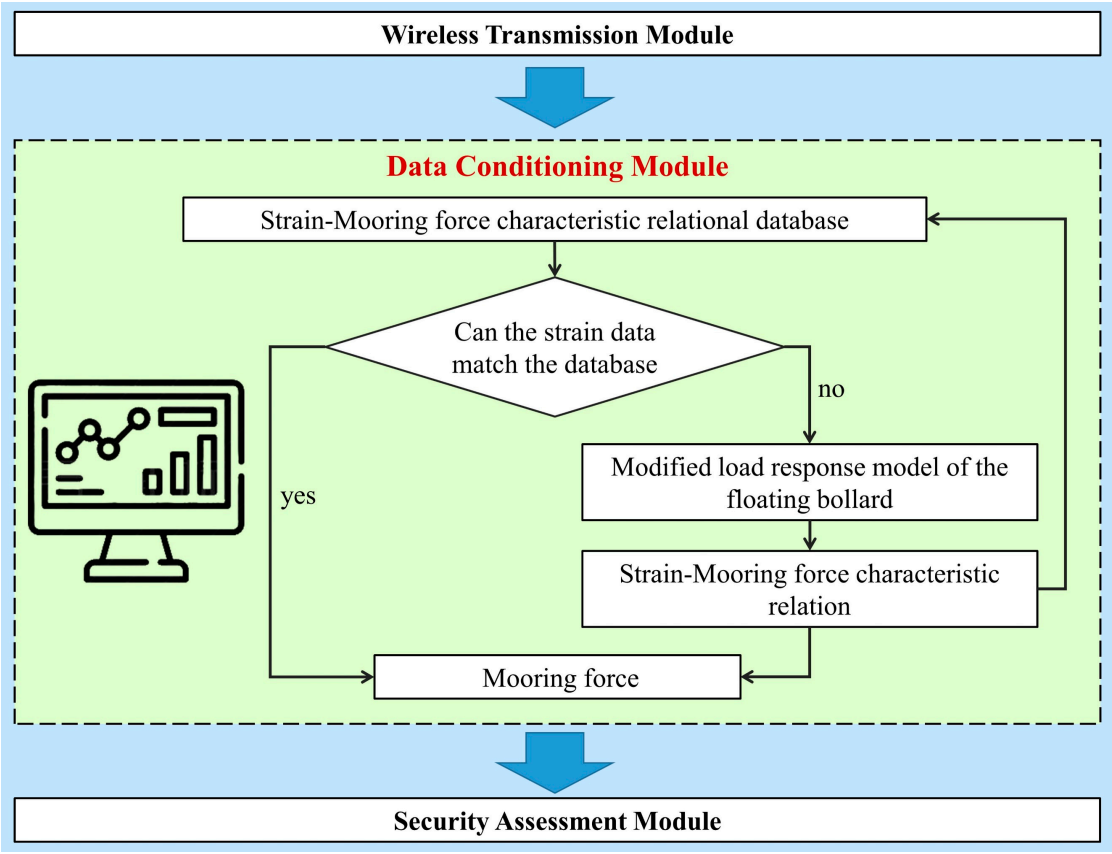

Figure 9. Data conditioning module's operating principle.

4.3.2. Data Storage Module

The data storage module stores key information, such as the strain amplitude spectrum and mooring force data in the data conditioning module, which can provide users with the query and download of the operation status and alarm historical data of the floating bollard.

4.3.3. Security Assessment Module

Based on the real-time mooring force determined by the modified load response model of the floating bollard, the designed permissible mooring force for the floating bollard in the ship lock is used as a quantitative index to evaluate the safety of the structure, and the threshold is determined via classification. By comparing the real-time mooring force with the early warning threshold, the dynamic state of the floating bollard structure is judged, and early warning is realized.

The early warning level of floating bollard safety can be divided into four levels according to factors such as the degree of harm that may be caused to the structure and the development trend.

(1) Level I: The measured mooring force exceeds 80% of the mooring force threshold, indicating that the situation is serious (red alert).

(2) Level II: The measured mooring force is 70~80% of the mooring force threshold, indicating that the situation is more urgent (orange alert).

(3) Level III: The measured mooring force is 60~70% of the mooring force threshold, indicating that the situation is generally urgent (yellow alert).

(4) Level IV: The measured mooring force is lower than 60% of the mooring force threshold, indicating that the floating bollard is in a safe state of operation (green safety indication).

Early warning information includes the alert level, starting time, occurrence location, warning matters, and measures to be taken, as shown in Figure 10.

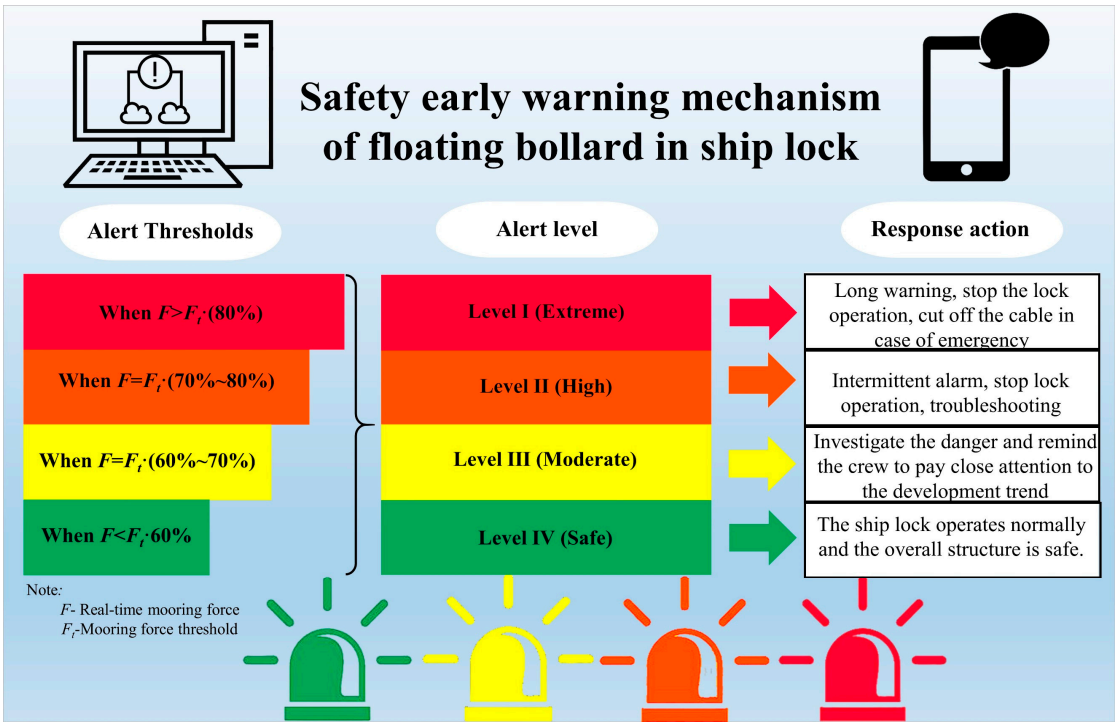

Figure 10. Early warning safety mechanism for floating bollards in ship locks.

4.4. Terminal Management System

The terminal management system includes a monitoring center and a user management module (see Figure 11). After receiving information on the ship's mooring force and the safety warning information of the operating status of the floating bollard, the monitoring center displays real-time information on the load condition, operating status, and warnings of the floating bollard. In the user management module, the user can use internet service to remotely control the equipment, which can realize the setting and management of a series of basic attributes, such as the number of locks and the number of floating bollards,

dynamics, monitoring indicators, and alarm strategies in the system. It can also retrieve, process, and analyze data anytime and anywhere.

Figure 11. System interface: (**a**) monitoring center; (**b**) basic attribute management module.

5. Field Test of the System

Based on a representative ship lock in China, a field test of a floating bollard with a real ship is carried out to obtain the strain duration data of the surface on the hollow cylinder body for the main structure of the floating bollard under a real ship mooring. After being transmitted to the intelligent monitoring system of the floating bollard in a ship lock, the ship mooring force is determined in real-time based on the modified load response model of the floating bollard. Combined with the actual values of the ship mooring force obtained via the field measurement using the tension sensor, the accuracy and operation effect of the intelligent monitoring system for a floating bollard in a ship lock developed in this paper are verified.

5.1. Test Procedure

According to the actual use of the floating bollard, a floating bollard with high mooring frequency, large berthing ship tonnage, and monitoring conditions is selected as the monitoring object. In this experiment, the No. 1 floating bollard on the right bank of the downstream side in the lock is determined as the measured object. According to the position of the measuring point, as depicted in Figure 3c, the strain gauge is fixed and installed in the monitoring point area, as shown in Figure 12a. To ensure the reliability of the long-term use of the strain monitoring sensor, a special stainless steel protective shell is installed outside the strain gauge, as shown in Figure 12b.

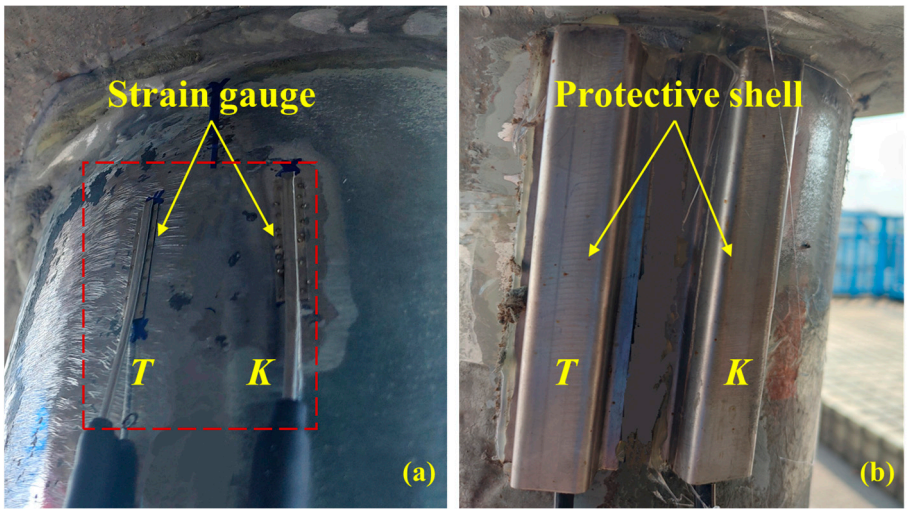

Figure 12. Sensor installation and protection: (**a**) strain gauge; (**b**) protective shell.

A typical inland waterway vessel is selected for the actual ship test. The lockage information of the vessel is shown in Table 3. After the vessel enters the lock chamber, a cable is hung on the target floating bollard, and the tension sensor is deployed on the cable to obtain the cable tension (mooring force) borne by the floating bollard structure during the whole process of the vessel passing through the lock in real-time, as shown in Figure 13. At the same time, the intelligent monitoring system of the floating bollard in the ship lock developed in this paper is used to synchronously measure the real-time strain data signal on the surface of the hollow cylinder of the floating bollard during the whole process and convert it into the numerical signal of the ship mooring force.

Table 3. Test vessel lock information.

Gross Tonnage (t)	Net Tonnage (t)	Quota Tonnage (t)	Overall Length (m)	Molded Breadth (m)	Molded Depth (m)
4712	3063	6635	110	17.2	5.6
Load draught (m)	Full-load displacement (t)	Light-load displacement (t)	Maximum ship height (m)	Actual draught (m)	Actual load tonnage (t)
4.9	7934	1224	17.5	3.7	4300

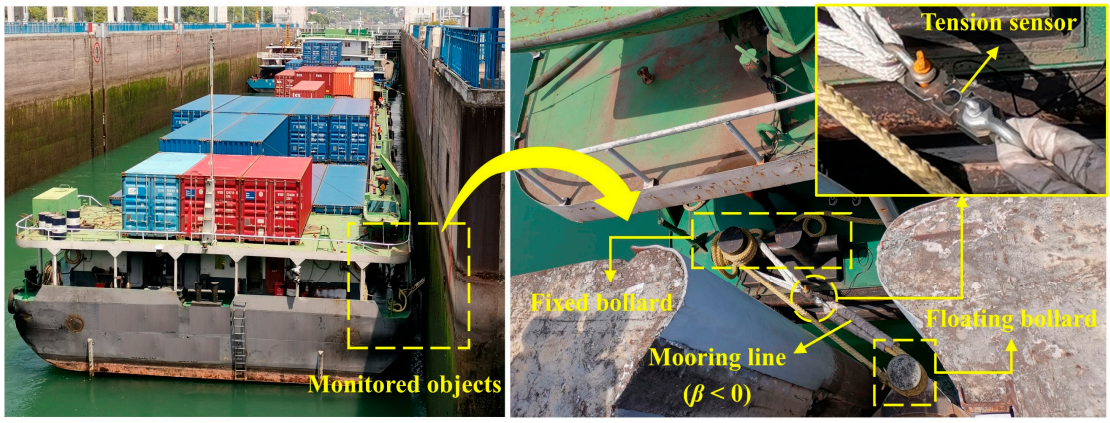

Figure 13. Field test.

5.2. Test Results and Analysis

During the real ship field test, the intelligent monitoring system of the floating bollard in the ship lock developed in this paper is used to monitor and display the real-time changing trend of the mooring force, i.e., F, as well as the mooring angle, i.e., α, for an actual ship; see Figure 14a. (Note: It is only used to show the operation effect.) When there is no ship load acting on the floating bollard, the system shows that the mooring force values of the floating bollard tend to be stable as a whole. When a ship load is applied to the floating bollard, the system detects a significant change in the mooring force. The maximum value of the mooring force can reflect the limit state of the mooring force and can intuitively show the force of the cable and the floating bollard in the instantaneous state.

The historical mooring force data of this test are obtained from the background of the system for statistical analysis. The maximum mooring force during the test is 64.35 kN, which is lower than the designed allowable mooring force of the floating bollard, which is 94.3 kN [34]. This suggests that the force state of the floating bollard structure is normal.

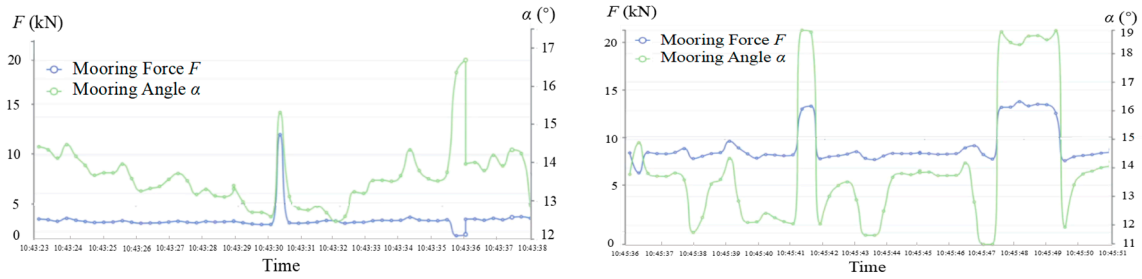

(**a**) Real-time action of mooring force and mooring angle.

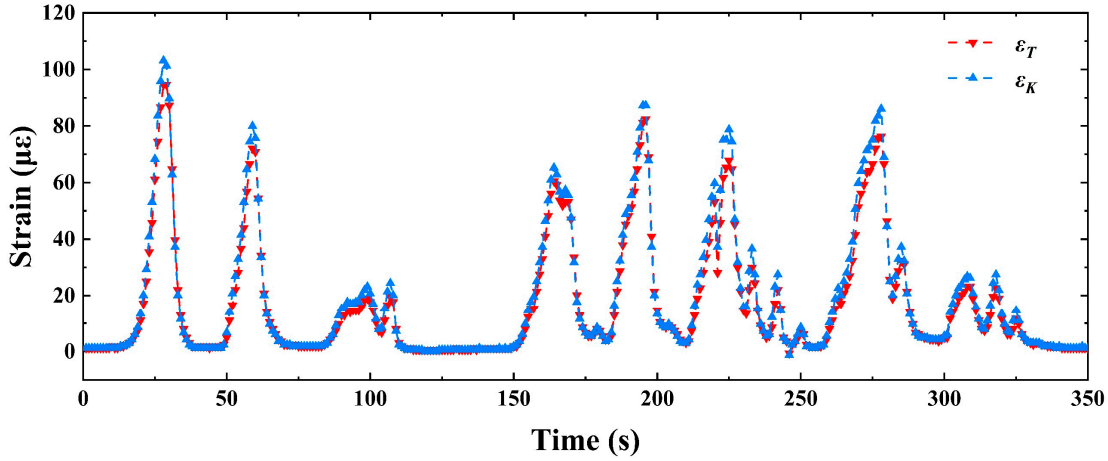

(**b**) Strain.

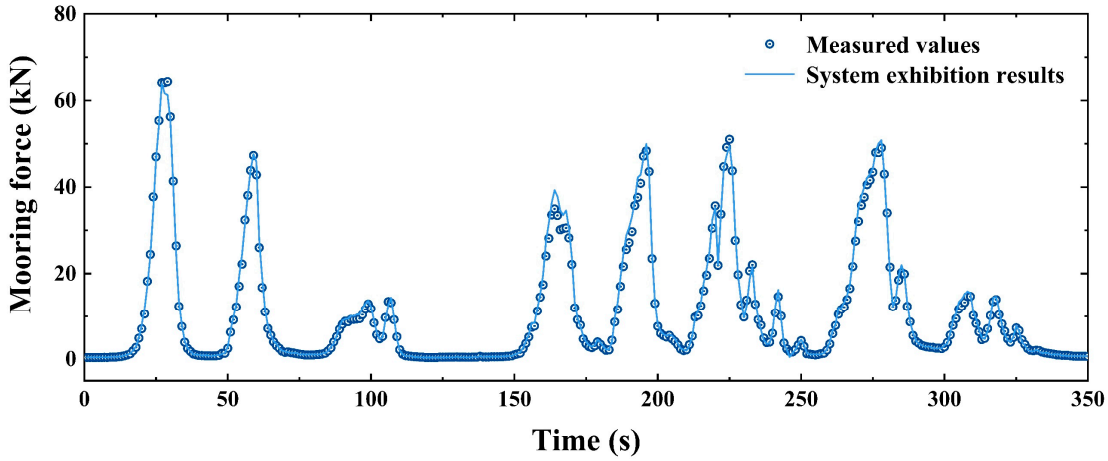

(**c**) Mooring force: system exhibition results vs. measured values.

Figure 14. Test results: (**a**) real-time action of mooring force; (**b**) strain; (**c**) mooring force: system exhibition results vs. measured values.

The time domain signal of the surface strain of the hollow cylinder of the floating bollard collected in the field test is interpreted and processed by means of filtering, noise reduction, and statistical analysis, and the effective strain duration data of the column surface of the test ship during the whole process of passing the lock are obtained, as shown in Figure 14b. (Note: The strain of a representative time period was selected for analysis.)

Based on the strain duration data of the surface of the floating bollard collected by the field ship test, combined with the modified load response model of the floating bollard built in the system, the real-time mooring force exerted on the floating bollard under the action of the real ship can be calculated. The results are compared with the measured values of the mooring force, and the results are shown in Figure 14c. In the figure, it can be

seen that the results of the mooring force based on the system display in this paper are in good agreement with the overall trend of the measured values.

To further quantify the difference between the calculated results of the modified load response model built into the system in this paper and the field test values, the relative error between the two is obtained via analysis, as shown in Figure 15. It can be seen in the figure that the relative error between the mooring force results based on the system and the measured values in the actual ship test are included in the range of ±15%, which fully verifies the evaluation accuracy of the intelligent monitoring system of floating bollards developed in this paper.

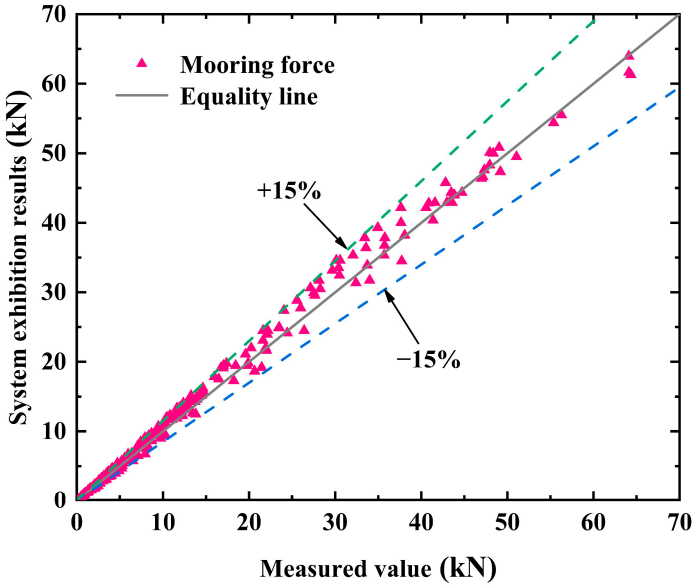

Figure 15. Relative error analysis: system exhibition results vs. measured values.

6. Discussion and Conclusions

On the basis of a theoretical model for the load response of a floating bollard, the theoretical model was modified based on a three-dimensional numerical simulation test of the main structure of the floating bollard, and the modified load response model of the floating bollard was constructed. With this model as the core, an intelligent monitoring system of a floating bollard in a ship lock was developed. The accuracy of the model and the operational effect of the system in this paper were further verified by a real ship field test. The specific conclusions are as follows:

(1) Numerical simulation experiments were carried out on the main structure of the floating bollard under multiple working conditions to analyze the error between the calculated values of the theoretical model of the floating bollard load response and the preset values of the numerical simulation experiments as influenced by different ship mooring forces F, vertical mooring angles β, and horizontal mooring angles α. The theoretical model was modified based on data from numerical simulation experiments. In conclusion, a modified load response model of the floating bollard was constructed.

(2) An intelligent monitoring system of a floating bollard in a ship lock utilizing modern technologies such as big data, internet, and cloud services was developed. The system was based on the modified load response model of the floating bollard and the hierarchical management mechanism of the early warning system of the floating bollard, which could effectively sense the load and operation status of the floating bollard in real-time.

(3) Relying on a representative ship lock in China, a field test of the operation effect of the intelligent monitoring system of the floating bollard in the ship lock was carried out. Through comparison and analysis, the relative error between the system calculated values of the mooring force and the field measurement values was 15%. It was thus

demonstrated that the monitoring system developed in this paper has the characteristics of high measurement accuracy and good signal stability, which can be further popularized and applied.

At present, the common floating bollard structure types in large ship lock engineering in China include the tripod type and the cylinder type. In this paper, the present study focuses solely on the research conducted on the tripod floating bollard structure, while the cylindrical floating bollard structure was not studied in depth. In future research, we will continue to improve the work of the intelligent monitoring system of the tripod floating bollard, and further carry out research related to the structure of the cylindrical floating bollard.

Author Contributions: Conceptualization, formal analysis, and methodology, L.W.; investigation, data curation, and writing—original draft, J.Y.; validation, Z.X.; supervision, M.L. (Mingwei Liu); writing—review and editing, M.L. (Minglong Li); software, Y.D.; resources, H.J. and C.D.; visualization, X.J. All authors have read and agreed to the published version of the manuscript.

Funding: This research was funded by the Science and Technology Innovation Project of Chongqing Education Commission (KJCX2020030), the Key Project of Technology Innovation and Application Development in Chongqing of China (CSTB2022TIAD-KPX0097), and the Research and Innovation Program for Graduate Students in Chongqing Jiaotong University (2023S0042).

Institutional Review Board Statement: Not applicable.

Informed Consent Statement: Not applicable.

Data Availability Statement: Data are contained within the article.

Conflicts of Interest: The authors declare no conflict of interest.

References

1. Passchyn, W.; Coene, S.; Briskorn, D.; Hurink, J.L.; Spieksma, F.C.R.; Vanden Berghe, G. The lockmaster's problem. *Eur. J. Oper. Res.* **2016**, *251*, 432–441. [CrossRef]
2. Ji, B.; Yuan, X.H.; Yuan, Y.B. Orthogonal Design-Based NSGA-III for the Optimal Lockage Co-Scheduling Problem. *IEEE Trans. Intell. Transp. Syst.* **2017**, *18*, 2085–2095. [CrossRef]
3. Sáenz, S.S.; Diaz-Hernandez, G.; Schweter, L.; Nordbeck, P. Analysis of the Mooring Effects of Future Ultra-Large Container Vessels (ULCV) on Port Infrastructures. *J. Mar. Sci. Eng.* **2023**, *11*, 856. [CrossRef]
4. Li, J.M.; Hu, Y.; Wang, X.; Diao, M.J. Operation safety evaluation system of ship lock based on extension evaluation and combination weighting method. *J. Hydroinform.* **2023**, *25*, 755–781. [CrossRef]
5. China Mocato. *Inland Navigation Structures of China*; China Communications Press: Beijing, China, 2021; pp. 9–19.
6. Jha, A.; Subedi, D.; Lovsland, P.O.; Tyapin, I.; Cenkeramaddi, L.R.; Lozano, B.; Hovland, G. Autonomous Mooring towards Autonomous Maritime Navigation and Offshore Operations. In Proceedings of the 15th IEEE Conference on Industrial Electronics and Applications (ICIEA 2020), Kristiansand, Norway, 9–13 November 2020; pp. 1171–1175.
7. Thorenz, C.; Bousmar, D.; Dubbelman, J.; Jun, L.; Spitzer, D.; Veldman, J.; Augustijn; Kortlever, W.; Hartley, A.J.R.; Moreno, A.; et al. PIANC Working Group 155 "Ship Behaviour in Locks and Lock Approaches". In Proceedings of the 33rd PIANC World Congress, San Francisco, CA, USA, 1–5 June 2014.
8. Zhou, Y.M.; Chu, X.M.; Jiang, Z.L.; Yu, Z. Research on Navigation Risk Identification of Three Gorges Ship Lock Based on Improved Analytic Hierarchy Process. In Proceedings of the 5th International Conference on Transportation Information and Safety (ICTIS), Liverpool, UK, 14–17 July 2019. [CrossRef]
9. Onishchenko, D.A.; Marchenko, A.V. Modelling of the passive turning of a turret moored vessel in conditions of compact ice. *Appl. Ocean Res.* **2019**, *90*, 101837. [CrossRef]
10. Van Zwijnsvoorde, T.; Vantorre, M.; Eloot, K.; Ides, S. Safety of container ship (un)loading operations in the Port of Antwerp Impact of passing shipping traffic. *Marit. Bus. Rev.* **2019**, *4*, 106–127. [CrossRef]
11. Sreedevi, R.; Nallayarasu, S. Investigation on ship mooring forces including passing ship effects validated by experiments. *Ocean Eng.* **2023**, *283*, 22. [CrossRef]
12. Nogueira, H.I.S.; van der Ven, P.; O'Mahoney, T.; De Loor, A.; van der Hout, A.; Kortlever, W. Effect of Density Differences on the Forces Acting on a Moored Vessel While Operating Navigation Locks. *J. Hydraul. Eng.* **2018**, *144*, 18. [CrossRef]
13. Hao, Q.; Zhang, J.; Zhu, X.; Liu, J. Responses of Large-ship Mooring Forces Based on Actual Measurement. *J. Ship Mech.* **2021**, *25*, 1685–1698. [CrossRef]
14. Yu, n.; Kim, S.-Y.; Lee, Y.-S. A Study on the Evaluation of Safety Stiffness from Ship's Mooring Bollards. *J. Korean Navig. Port Res.* **2019**, *43*, 9–15. [CrossRef]

15. Yibing, W.; Jianfeng, w.; Yafei, C.; Huafeng, T. Numerical Simulation and Analysis of Static Response of Ship Bitts. *Navig. China* **2015**, *38*, 87–91.
16. Wu, J.; Shu, Y.; Zhou, S.; Bai, L.; Cao, S. Structure monitoring mothod and experiment of large-scale wharf bollards. *Opt. Precis. Eng.* **2021**, *29*, 1631–1639. [CrossRef]
17. De Mulder, T. Mooring forces and ship behaviour in navigation locks. *Innov. Navig. Lock Des.* **2009**, *15*, 17.
18. Liu, M.; Zeng, L.; Qi, J.; Jiang, T. Numerical simulation of stress state of floating bollards of ship lock. *Port Waterw. Eng.* **2020**, *12*, 112–117. [CrossRef]
19. Liu, M.; Wang, Z.; Wu, L.; Li, M.; Yang, J. Safety monitoring method for mooring lines of floating bollards in ship lock. *Port Waterw. Eng.* **2023**, *3*, 85–91. [CrossRef]
20. Liu, M.; Li, M.; Wu, L.; Jiang, T.; Zhao, D. Mechanical Model of Load-Bearing Response of Floating Bollard of Ship Lock. *J. Chongqing Jiaotong Univ.* **2022**, *41*, 127–132. [CrossRef]
21. Wu, L.; Xiang, Z.; Shu, D.; Liu, M.; Yang, J.; Li, M. Dynamic Inversion Model of the Mooring Force on a Floating Bollard of a Sea Lock. *J. Mar. Sci. Eng.* **2023**, *11*, 1374. [CrossRef]
22. Qi, J.; Li, L.; Jiang, T.; Xiang, Z.; Yang, J.; Wu, L. Structural load monitoring of floating mooring column and its application on optimal regulation for water conveyance system operation of sea shiplock. *Front. Energy Res.* **2023**, *11*, 1218430. [CrossRef]
23. Chen, C.; Li, Y. Real-time tracking and dynamic berthing information extraction system with 2D LiDAR data. *Ocean Eng.* **2023**, *276*, 114181. [CrossRef]
24. Feng, L.; Si-jie, W.; Yu-shan, W.; Xiao-fei, W. Design of Wireless Monitoring and Warning System for Mooring Line Tension. *Navig. China* **2013**, *42*, 196–199.
25. Li, R.; Zhang, J.; Xiao, J.B. Operation State Evaluation of Miter Gate Based on On-Line Monitoring and Finite Element Analysis. *Appl. Sci.* **2023**, *13*, 13. [CrossRef]
26. Zhang, P.P.; Wang, W.; Zhou, J.H.; Jiang, Y.S.; Chen, X. Research on the Condition Monitoring of the Reverse Tainter Valve in Ship Locks. In Proceedings of the Prognostics and System Health Management Conference (PHM-Besancon), Besancon, France, 4–7 May 2020. [CrossRef]
27. Tang, W.; Zhang, P.; Liu, Y.; Wang, L.H.; Liu, L.F. Shiplock Multi-Channel Water Level Monitoring and Message Interaction. *Appl. Mech. Mater.* **2013**, *321–324*, 586–591. [CrossRef]
28. Misovic, D.S.; Milic, S.D.; Durovic, Z.M. Vessel Detection Algorithm Used in a Laser Monitoring System of the Lock Gate Zone. *IEEE Trans. Intell. Transp. Syst.* **2016**, *17*, 430–440. [CrossRef]
29. Liu, C.; Qi, J.; Chu, X.; Zheng, M.; He, W. Cooperative ship formation system and control methods in the ship lock waterway. *Ocean Eng.* **2021**, *226*, 108826. [CrossRef]
30. Yan, H.; Yin, Q.Z.; Rao, K.P.; Liu, X.T. Design and Research of Ship Carrier for Three Gorges New Ship Locks. In Proceedings of the 4th International Conference on Advances in Energy Resources and Environment Engineering (ICAESEE), Chengdu, China, 7–9 December 2018; Available online: https://iopscience.iop.org/article/10.1088/1755-1315/237/3/032111 (accessed on 31 August 2023).
31. Hu, Q.; Lin, L.S.; Qui, Y.P. Design and Implementation of Ship Through Lock in River Management System Based on RFID. In Proceedings of the International Conference on Information Technology and Management Innovation (ICITMI2012), Guangzhou, China, 10–11 November 2012. [CrossRef]
32. Technical Management Office of Water Transport Planning and Design Institute. General design specification for mooring post members. *Port Waterw. Eng.* **1978**, *12*, 3–17.
33. Chen, Z. Research on Large-scale Ship Parameters Based on Mooring Safety in Three Gorges Ship Lock. Master's Thesis, Wuhan University of Technology, Wuhan, China, 2017.
34. CCCC Water Transportation Consultants Co., Ltd. *Code for Master Design of Shiplocks*; Ministry of Transport of the People's Republic of China: Beijing, China, 2001.